



## ORIGINAL ARTICLE

# Green synthesis of palladium nanoparticles using gum ghatti (*Anogeissus latifolia*) and its application as an antioxidant and catalyst



Aruna Jyothi Kora \*, Lori Rastogi

National Centre for Compositional Characterisation of Materials (NCCCM), Bhabha Atomic Research Centre, ECIL PO, Hyderabad 500 062, India

Received 16 March 2015; accepted 17 June 2015  
Available online 24 June 2015

## KEYWORDS

Antioxidant;  
Catalyst;  
Green synthesis;  
Gum ghatti;  
Palladium nanoparticles;  
Dye degradation

**Abstract** A facile and green route for the synthesis of palladium nanoparticles from palladium chloride was developed using non-toxic, renewable plant polymer, gum ghatti (*Anogeissus latifolia*), as both the reducing and stabilizing agent. The generated nanoparticles were characterized with UV–visible spectroscopy (UV–vis), dynamic light scattering (DLS), transmission electron microscopy (TEM), and X-ray diffraction (XRD) techniques. The formation of palladium nanoparticles was confirmed from the appearance of intense brown colour and broad continuous absorption spectra in the UV–visible region. The produced nanoparticles were found to be spherical in shape, poly-disperse and the average particle size was  $4.8 \pm 1.6$  nm. The face centred cubic crystal structure of the fabricated nanoparticles is confirmed from the selected-area electron diffraction and XRD patterns. Compared to earlier reports, the nanoparticles showed superior antioxidant at a much lower nanoparticle dose. Also, the homogenous catalytic activity of palladium nanoparticles was studied by probing the reduction of dyes such as coomassie brilliant blue G-250, methylene blue, methyl orange, and a nitro compound, 4-nitrophenol with sodium borohydride. The nanoparticles exhibited excellent catalytic activity in dye degradation and the results of this study demonstrate the possible application of biogenic palladium nanoparticles as nanocatalyst in environmental remediation. © 2015 The Authors. Production and hosting by Elsevier B.V. on behalf of King Saud University. This is an open access article under the CC BY-NC-ND license (<http://creativecommons.org/licenses/by-nc-nd/4.0/>).

\* Corresponding author. Tel.: +91 40 2712 1365; fax: +91 40 2712 5463.

E-mail addresses: [koramaganti@gmail.com](mailto:koramaganti@gmail.com) (A.J. Kora), [lorirastogi@gmail.com](mailto:lorirastogi@gmail.com) (L. Rastogi).

Peer review under responsibility of King Saud University.



Production and hosting by Elsevier

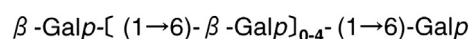
## 1. Introduction

Palladium nanoparticles are routinely used as catalysts in various organic transformations including Suzuki-cross coupling, Mizoroki-Heck, Stille and Sonogashira coupling reactions (Rao et al., 2006). In addition to their use as homogeneous or heterogeneous catalyst (Kim et al., 2002), nanoparticles of palladium are widely used in many applications such as hydrogen storage (Hakamada et al., 2011), hydrogen sensor

(Mubeen et al., 2007), chemical modifier in ETV-ICP-MS (Hsu et al., 2013), automotive catalytic converter, chemo-optical transducers, plasmonic wave guides, and optical limiting devices (Meena Kumari et al., 2013). The biogenic synthesis of metallic nanoparticles has gained considerable attention in the recent times as a viable option to physical and chemical methods, due to the adaptation of most of the green chemistry principles (Anastas and Warner, 1998). This is chiefly due to the innate abundance of renewable, cheap and biodegradable materials of biological origin from a vast variety of resources (Iravani, 2011). In the case of palladium nanoparticles, bacteria such as *Plectonema boryanum* (Lengke et al., 2007), *Shewanella oneidensis* (Ogi et al., 2011) and *Geobacter sulfurreducens* (Tuo et al., 2013) were used. While plant sources including the extracts from fruit (*Gardenia jasminoides* (Lishan et al., 2009), bark (*Cinnamom zeylanicum*) (Sathishkumar et al., 2009), peels (banana (Bankar et al., 2010), *Annona squamosa* (Roopan et al., 2012)) and root (*Asparagus racemosus*) (Raut et al., 2013) were extensively used for palladium nanoparticle synthesis. The leaf extracts from various plants including *Solanum trilobatum* (Kanchana et al., 2010), *Anacardium occidentale* (Sheny et al., 2012), *Catharanthus roseus* (Kalaiselvi et al., 2015) were also utilized for the production of palladium nanoparticles. The catalytic activity of various metallic nanoparticles such as silver (Bindhu and Umadevi, 2015; Kundu, 2013; Narayanan et al., 2013), gold (Maity et al., 2012; Narayanan and Sakthivel, 2011; Praharaj et al., 2004; Sen et al., 2013), palladium (Dauthal and Mukhopadhyay, 2013; Kalaiselvi et al., 2015; Santoshi Kumari et al., 2015), platinum (Coccia et al., 2012) and iridium (Kundu and Liang, 2011) was widely studied in reduction of various dyes.

In this perspective, we have developed a facile and green route for the synthesis of palladium nanoparticles from palladium chloride using non-toxic, renewable natural plant polymer of Indian origin: gum ghatti (*Anogeissus latifolia*) as both the reducing and stabilizing agent. The exudate tree gum was chosen to explore its potential for bioprospecting applications in palladium nanoparticle production. Gum ghatti is an arabinogalactan type of natural biopolymer with well characterized morphological, structural, physico-chemical, compositional, solution, rheological and emulsifying properties. The primary structure of this gum contains sugars such as arabinose, galactose, mannose, xylose and glucuronic acid. The gum contains alternating 4-*O*-substituted and 2-*O*-substituted  $\alpha$ -D-mannopyranose units and chains of 1  $\rightarrow$  6 linked  $\beta$ -D-galactopyranose units with side chains of L-arabinofuranose residues. 6% of rhamnose in the polysaccharide is linked to the galactose backbone as  $\alpha$ -Rhap-(1  $\rightarrow$  4)  $\beta$ -galactopyranose side chain (Fig. 1) (Tischer et al., 2002). Also, it is an approved food ingredient by the Food and Drug Administration, USA, and its application in food is permitted in many countries such as Australia, China, Iran, Japan, Latin America, Russia, Saudi Arabia, Singapore, South Africa and South Korea. It is considered as a food grade additive by the Bureau of Indian Standards, India, under Indian Standard IS 7239:1974. It is extensively used as a binder, emulsifier, flavour fixative, stabilizer and thickener in alcoholic beverages, carbonated drinks, chewing gums, creams, oil and aqueous emulsions and syrups (Amar et al., 2006; Kaur et al., 2009).

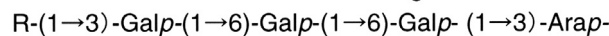
#### • main chain structures



#### • others

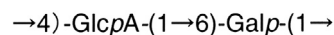
↓

3



4

↑



3

↑

**Figure 1** The assigned structure of gum ghatti (Tischer et al., 2002).

In the present study, we have characterized the biogenic, gum ghatti synthesized palladium nanoparticles with various techniques for particle morphology, size, hydrodynamic diameter, crystal structure, etc. The nanoparticles were investigated for their antioxidant and antibacterial activities. We have also evaluated the homogenous catalytic ability of the green palladium nanoparticles by studying the degradation of various dyes.

## 2. Materials and methods

### 2.1. Synthesis of palladium nanoparticles

Palladium chloride ( $\text{PdCl}_2$ ), sodium borohydride ( $\text{NaBH}_4$ ), 4-nitrophenol, methylene blue, coomassie brilliant blue G-250 and methyl orange of analytical reagent grade were used. All the solutions were prepared in ultra pure water. "Gum ghatti", grade-I was purchased from Girijan Co-operative Corporation Ltd., Hyderabad, India. The gum was powdered in a Prestige Deluxe-Vs high speed mechanical blender (Bengaluru, India) and sieved to obtain a particle size of 38  $\mu\text{m}$ . Then, a 0.5% (w/v) of homogenous gum stock solution was prepared in ultrapure water by stirring overnight at room temperature. Then, this solution was centrifuged (5500 $\times$ g, 10 min) to remove the insoluble materials and the supernatant was used for synthesis. The palladium nanoparticles were synthesized by autoclaving the gum solutions containing  $\text{PdCl}_2$  at 121  $^\circ\text{C}$  and 103 kPa for 30 min. The effect of variations of concentrations of gum (0.1–0.5%) and palladium chloride (0.125–1.0 mM) on nanoparticle synthesis was also studied.

### 2.2. Characterization of synthesized palladium nanoparticles

The UV–visible absorption spectra of the prepared palladium nanoparticle solutions were recorded using Biotek Synergy<sup>TM</sup> H1 microplate reader (Winooski, Vermont, USA), from 300 to 800 nm, against autoclaved gum blanks. The  $z$ -average particle size, particle size distribution and polydispersity index (PDI) of the produced palladium nanoparticles were assessed with a dynamic light scattering (DLS) device Malvern Zetasizer Nano ZS90 (Malvern, UK). The size and shape of the nanoparticles were obtained with FEI Tecnai 20 G2

S-Twin (Eindhoven, The Netherlands) transmission electron microscope (TEM), operating at 200 kV. The size of a minimum of 100 particles was measured and their size distribution, mean diameter and standard deviation were obtained using OriginPro 7.0 software. The samples for TEM were prepared by depositing a drop of colloidal solution on a carbon coated copper grid and drying at room temperature. The X-ray diffraction analysis was conducted with a Rigaku, Ultima IV diffractometer (Tokyo, Japan) using monochromatic Cu K $\alpha$  radiation ( $\lambda = 1.5406 \text{ \AA}$ ) running at 40 kV and 30 mA. The intensity data for the nanoparticle solution deposited on a glass slide were collected over a  $2\theta$  range of  $30\text{--}100^\circ$  with a scan rate of  $1^\circ/\text{min}$ .

### 2.3. Antioxidant activity of synthesized palladium nanoparticles

The antioxidant activity of the nanoparticles synthesized with 0.5% gum at 0.75 mM PdCl<sub>2</sub> conc. was studied by scavenging (1'-1' diphenyl picryl-hydrazyle) (DPPH), a stable free radical with purple colour. The wells of a flat bottom, polystyrene microtitre plate were loaded with 100  $\mu\text{M}$  of DPPH prepared in absolute ethanol at 1–15  $\mu\text{g}/\text{mL}$  concentration of nanoparticles (0.75 mM, 2.5–37.5  $\mu\text{L}$ ) and incubated in dark at room temperature for 60 min. The negative controls were maintained with DPPH and autoclaved gum, respectively. The plate wells loaded with 50  $\mu\text{g}/\text{mL}$  of ascorbic acid were used as positive control. The absorbance at 520 nm was recorded and the scavenging percentage of DPPH was calculated using the formula: DPPH scavenging (%) = (DPPH absorbance – sample absorbance/DPPH absorbance)  $\times$  100.

### 2.4. Catalytic activity of synthesized palladium nanoparticles

The catalytic activity of palladium nanoparticles generated with 0.5% gum and 0.75 mM PdCl<sub>2</sub> at 3.2  $\mu\text{g}/\text{mL}$  concentration (0.75 mM–40  $\mu\text{L}$ ) was determined by studying the reduction of three chemical dyes: coomassie brilliant blue G-250 (CBB), methylene blue (MB) and methyl orange (MO) and a nitro compound, 4-nitrophenol (4-NP) with sodium borohydride (NaBH<sub>4</sub>) at 12.5 mM concentration (500 mM–25  $\mu\text{L}$ ), as a model reaction. The degradation was investigated by measuring the UV–vis spectra. The control reactions were monitored in the absence of NaBH<sub>4</sub> and palladium nanoparticles. The negative control was also included with autoclaved gum and NaBH<sub>4</sub> solutions.

### 2.5. Antibacterial activity of synthesized palladium nanoparticles

The antibacterial activity of the synthesized nanoparticles at 0.5% gum and 0.75 mM PdCl<sub>2</sub> conc. was determined with well diffusion method (Kora et al., 2012). *Pseudomonas aeruginosa* (ATCC 27853) and *Staphylococcus aureus* (ATCC 25923) were used as test strains representing Gram-negative and Gram-positive bacteria, respectively. The bacterial suspension was prepared from overnight grown culture in nutrient broth by adjusting the turbidity to 0.5 McFarland standard. Mueller Hinton agar plates were inoculated with this bacterial suspension and 125  $\mu\text{L}$  of 0.75 mM concentration of nanoparticle solution containing 10  $\mu\text{g}$  of palladium was added to the 8 mm diameter well. The negative control was maintained with autoclaved gum blank and the culture plates loaded with 10  $\mu\text{g}$

of antibiotic streptomycin were included as positive control. These plates were incubated at 37  $^\circ\text{C}$  for 24 h in a bacteriological incubator and the zone of inhibition (ZOI) was measured by subtracting the well diameter from the total inhibition zone diameter. Three independent experiments were carried out with each bacterial strain.

## 3. Results and discussion

### 3.1. UV–visible spectroscopy (UV–vis)

The palladium nanoparticle formation was examined visually and by UV–vis. After autoclaving, the colour of reaction mixture changed from pale yellow to dark brown, an evidence for the formation of palladium nanoparticles by the gum (Inset (I) of Fig. 2(a)). Further, the nanoparticle synthesis was

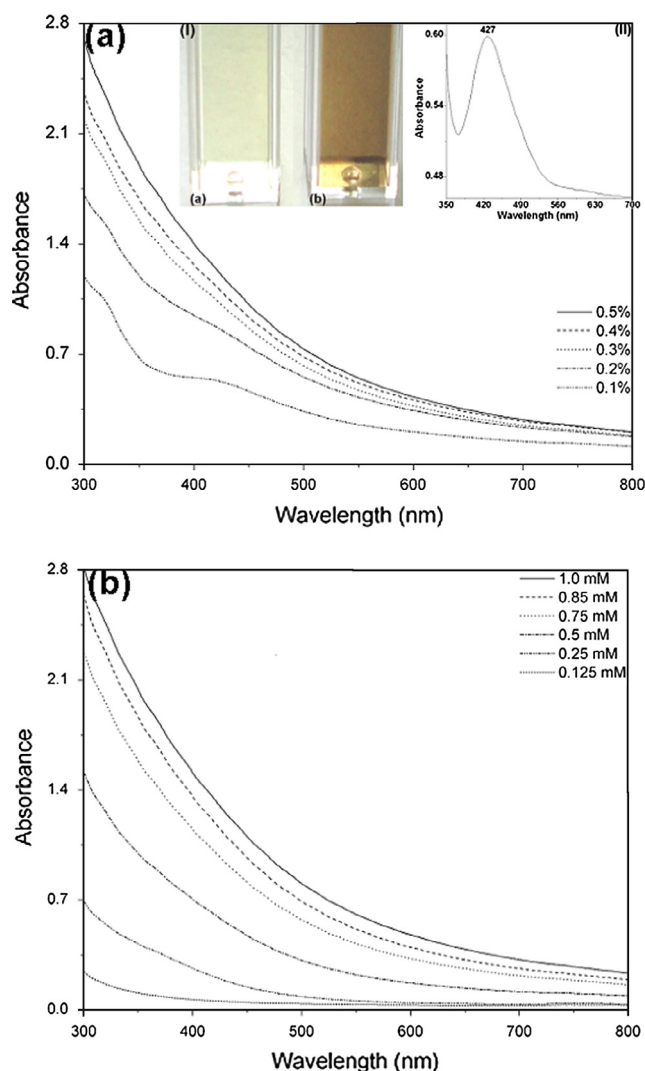


**Figure 2** The UV–vis absorption spectra of palladium nanoparticles synthesized by 30 min of autoclaving with (a) different concentrations of gum (0.1–0.5%) at 1 mM PdCl<sub>2</sub> concentration. Inset: (I) colour of the reaction mixture at 0.5% gum (a) before and (b) after autoclaving and (II) the absorption spectrum of 1 mM PdCl<sub>2</sub> solution; and (b) different concentrations of PdCl<sub>2</sub> (0.125–1.0 mM).

monitored by recording the absorption spectra of synthesized colloidal solutions, against respective blanks. The aqueous 1 mM PdCl<sub>2</sub> blank solution showed a discrete absorption peak at 427 nm, indicating the presence of Pd<sup>2+</sup> ions (Inset (II) of Fig. 2(a)). Upon autoclaving with gum, the characteristic absorption peak was changed to a broad continuous absorption spectrum (Fig. 2(a)). Thus, these continuous absorption spectra in the UV–visible region indicate the formation of palladium nanoparticles of less than 10 nm size. These results are in accordance with the previous studies on synthesis of palladium nanoparticles using *A. occidentale* leaf powder (Sheny et al., 2012) and tannic acid (Meena Kumari et al., 2013). The synthesis was studied by varying the gum concentration (0.1–0.5%) at 1 mM PdCl<sub>2</sub> for 30 min of autoclaving (Fig. 2(a)). With an increase in gum concentration, there is an enhancement in the reduction of palladium ions. The reduction was evaluated for 30 min by varying the PdCl<sub>2</sub> concentration (0.125–1.0 mM) at 0.5% gum (Fig. 2(b)). It was observed that the intensity of the absorption band increased with an increase in metal precursor concentration, possibly due to the formation of larger particles at higher concentration. At a higher concentration of 1 mM PdCl<sub>2</sub>, the produced colloidal solutions were not stable and aggregated within a day. These observations indicate the lack of stabilization of process between capping molecules and surfaces of the nanoparticles at a higher palladium concentration.

During autoclaving, due to the expansion of biopolymer the available functional groups on the gum become more accessible for palladium ions. The gum has been categorized under arabinogalactan due to the abundance of arabinose and galactose and known to be rich in uronic acid content (Amar et al., 2006; Kaur et al., 2009). The hydroxyl and carboxylic groups of the gum complex the palladium ions which can be further reduced to elemental palladium by the reducing aldehyde groups. Then, these nanoparticles are possibly capped and stabilized by the proteins and polysaccharides of the gum (Kora et al., 2012).

The superiority of the present method over other earlier reports was justified by comparing the other biogenic synthetic protocols for palladium nanoparticles (Table 1). With many extract based protocols including *C. roseus* (Kalaiselvi et al., 2015), *A. squamosa* (Roopan et al., 2012), *G. jasminoides* (Lishan et al., 2009), the rate of reaction is slow at 60 °C and the time required for the reduction of palladium ions varied from 2 to 24 h for the generation of nanoparticles sized around 38 nm, 100 nm and 3–5 nm, respectively. Whereas, using banana peel at the same temperature, nanoparticles are produced within 3 min, but are of higher size of 50 nm (Bankar et al., 2010). Protocols based on nanoparticle synthesis at room temperature using extracts of *S. trilobatum* (Kanchana et al., 2010) and *C. zeylanicum* (Sathishkumar et al., 2009); nanoparticles sized around 60–100 nm and 15–20 nm are produced at an incubation time of 24–72 h, respectively. In previous studies on bacterial based nanoparticle synthesis at room temperature using *S. oneidensis* (Ogi et al., 2011) and *G. sulfurreducens* (Tuo et al., 2013), supply of electron donor and acceptors; and anaerobic conditions are required for the production of nanoparticles of 5–10 nm. While in this work, palladium nanoparticles of 4.8 nm size were produced within 30 min at 121 °C. This observation supports the advantage of the current synthetic protocol over earlier reported biosynthetic methods.

**Table 1** Comparison of biogenic palladium nanoparticles synthesized by green methods.

Biological entity	Reaction conditions	Average size (nm)	References
Gum ghatti ( <i>Anogeissus latifolia</i> )	121 °C, 30 min	4.8	Present study
<i>Annona squamosa</i> peel	60 °C, 4 h	100	Roopan et al. (2012)
<i>Solanum trilobatum</i> leaf extract	Room temperature, 24 h	60–100	Kanchana et al. (2010)
Banana peel	80 °C, 3 min	50	Bankar et al. (2010)
<i>Catharanthus roseus</i> leaf extract	60 °C, 2 h	38	Kalaiselvi et al. (2015)
<i>Plectonema boryanum</i>	25–100 °C, 28 day	≤30	Lengke et al. (2007)
<i>Cinnamom zeylanicum</i> bark extract	30 °C, 72 h	15–20	Sathishkumar et al. (2009)
<i>Shewanella oneidensis</i>	Room temperature, 1 h, anaerobic, electron donor	5–10	Ogi et al. (2011)
<i>Geobacter sulfurreducens</i>	Room temperature, 3 h, anaerobic, electron donor and acceptor	5–10	Tuo et al. (2013)
<i>Gardenia jasminoides</i> fruit extract	60 °C, 24 h	3–5	Lishan et al. (2009)

### 3.2. Mean particle size and polydispersity index (PDI)

The DLS technique was used to optimize the nanoparticle synthesis by determining the mean particle size and PDI. With an increase in gum concentration from 0.1% to 0.5%, the mean particle size and PDI decreased at 1 mM concentration of PdCl<sub>2</sub> and 30 min autoclaving (Fig. 3(a)). Further, the particle size distribution was evaluated by varying the PdCl<sub>2</sub> concentration (0.125–1.0 mM) at 0.5% gum. With an increase in metal precursor concentration, the diameter and PDI decreased sharply till 0.75 mM and then increased at 0.85 and 1.0 mM PdCl<sub>2</sub> (Fig. 3(b)). At a higher palladium concentration of 1.0 mM, the rate of nuclei formation and nanoparticle collision is higher compared to the rate of nanoparticle capping by the function groups of the gum. Based on the observations, the optimal conditions for palladium nanoparticle synthesis were found to be 0.5% gum, 0.75 mM PdCl<sub>2</sub> with 30 min of autoclaving. At optimal synthesis conditions, the average particle diameter was found to be around 74.8 nm.

### 3.3. Transmission electron microscopy (TEM)

The TEM images of palladium nanoparticles (Pd NP) synthesized at optimum conditions of 0.5% gum, 0.75 mM PdCl<sub>2</sub> with 30 min of autoclaving are shown in Fig. 4. The produced nanoparticles were spherical in shape; size of the particles ranged from 2.3 to 7.5 nm and the average particle size obtained

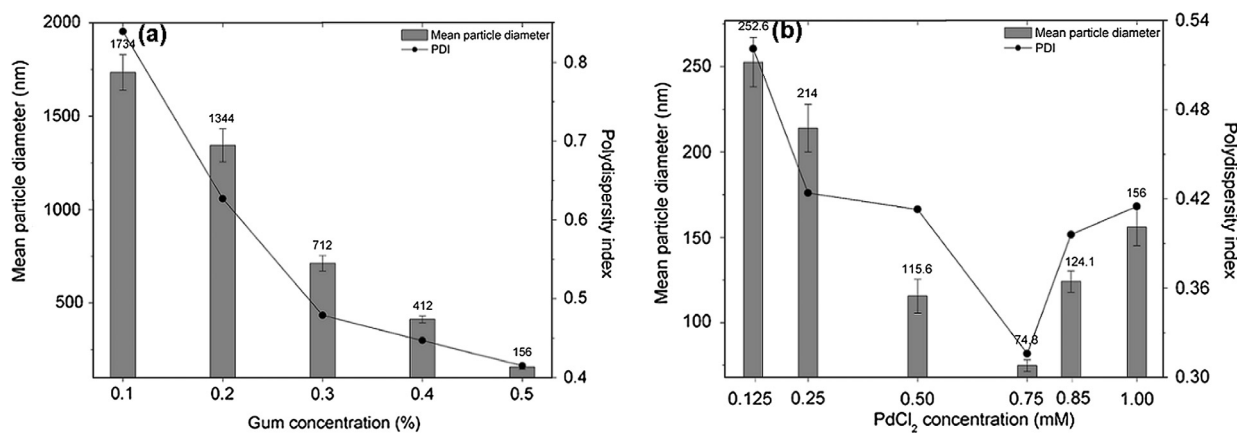


**Figure 3** The mean particle diameter and polydispersity of index of palladium nanoparticles as a function of (a) gum concentration at 1 mM PdCl<sub>2</sub> and (b) PdCl<sub>2</sub> concentration at 0.5% gum.

from the corresponding diameter distribution was about  $4.8 \pm 1.6$  nm (Fig. 4(e)). The selected-area electron diffraction (SAED) pattern given in Fig. 4(d) exhibits concentric rings with intermittent bright spots, confirm a highly crystalline nature of the produced nanoparticles. These rings can be attributed to the diffraction from the (111), (200) and (220) planes of face centred cubic (fcc) palladium. The crystallinity of the synthesized nanoparticles was also substantiated from the observed clear lattice fringes in high-resolution image (Fig. 4(c)). With the same nanoparticles synthesized at optimal conditions, the DLS showed higher particle size compared to TEM. DLS provides information on hydrodynamic diameter of the particles which includes inorganic core plus molecules adsorbed on the surface, whereas TEM gives the true radius of the particles. Thus, the reported higher size in DLS is due to capping of nanoparticles by protein and polysaccharide molecules of the gum.

### 3.4. X-ray diffraction (XRD)

The crystal structure of the produced nanoparticles was determined by XRD. There were five well-defined characteristic diffraction peaks at  $40.1^\circ$ ,  $46.7^\circ$ ,  $68.1^\circ$  and  $82.2^\circ$ , respectively, indexed to reflections from (111), (200), (220) and (311) planes of face centred cubic (fcc) crystal structure of metallic palladium (Fig. 5). The interplanar spacing ( $d_{hkl}$ ) values (2.246, 1.943, 1.375 and 1.171 Å) and the lattice constant (3.886 Å) calculated from the XRD spectrum of palladium nanoparticles are in agreement with the standard palladium values (JCPDS PDF card 46-1043). Thus, the XRD pattern further substantiates the highly crystalline nature of nanoparticles observed from selected-area electron diffraction (SAED) pattern depicting concentric rings (Fig. 4). Also, the effect of nano-sized particles was shown in a broadening of the diffraction peaks. The relative intensities of (200) to (111) and (220) to (111) planes are much lower than the standard values (0.32 against 0.6 and 0.17 against 0.42). From these data, it is clear that (111) lattice plane is the favoured orientation for the generated nanoparticles (Meena Kumari et al., 2013; Shen et al., 2012). The calculated particle size of the crystalline nanoparticles using Scherrer's formula is

7.06 nm, which is matching well with the TEM results within the limitations of the formula.

### 3.5. Antioxidant activity

The antioxidant potential of the green synthesized Pd NP was evaluated by quantifying the DPPH free radical scavenging activity (Fig. 6). In the presence of nanoparticles, the colour of the DPPH solution gradually changed from purple to pale yellow with time. The percentage scavenging of DPPH increased linearly with an increase in nanoparticle concentration from 1 to 15 µg/mL and reached 81.9% within 60 min at 15 µg/mL. While, the positive control ascorbic acid showed 94.0% of scavenging activity at a concentration of 50 µg/mL. The negative control wells loaded with autoclaved gum did not show any colour change from purple. Nanoparticles of silver, gold (Ramamurthy et al., 2013), selenium (Kong et al., 2014), nickel oxide (Saikia et al., 2010) and copper oxide (Das et al., 2013) are known to exhibit free radical scavenging activity. To further evaluate the results, we have compared our values with other metal and metal oxide nanoparticles (Table 2). In a study carried out with biologically synthesized silver and gold nanoparticles of 5–50 nm size, DPPH scavenging activity of 55% and 50%, was reported at a particle concentration of 250 µg/mL, respectively (Ramamurthy et al., 2013). In another study carried out with gum arabic-stabilized selenium nanoparticles sized around 34.9 nm, DPPH scavenging activity of 85.3% was reported at a particle concentration of 4 mg/mL (Kong et al., 2014). A DPPH scavenging activity of 85% was noted in an earlier evaluation study carried out with 15–30 nm sized copper oxide nanoparticles synthesized by the thermal decomposition method, at 37.5 mg/mL of nanoparticles (Das et al., 2013). With nickel oxide nanoparticles of 12–23 nm at 33.3 mg/mL concentration of nanoparticles, a DPPH scavenging activity of 90% was noted (Saikia et al., 2010). While in this study, DPPH scavenging activity of 81.9% was observed at 15 µg/mL of 4.8 nm sized palladium nanoparticles. The data confirm the dependency of antioxidant activity on particle size and concentration. Thus, the present report demonstrates the superior

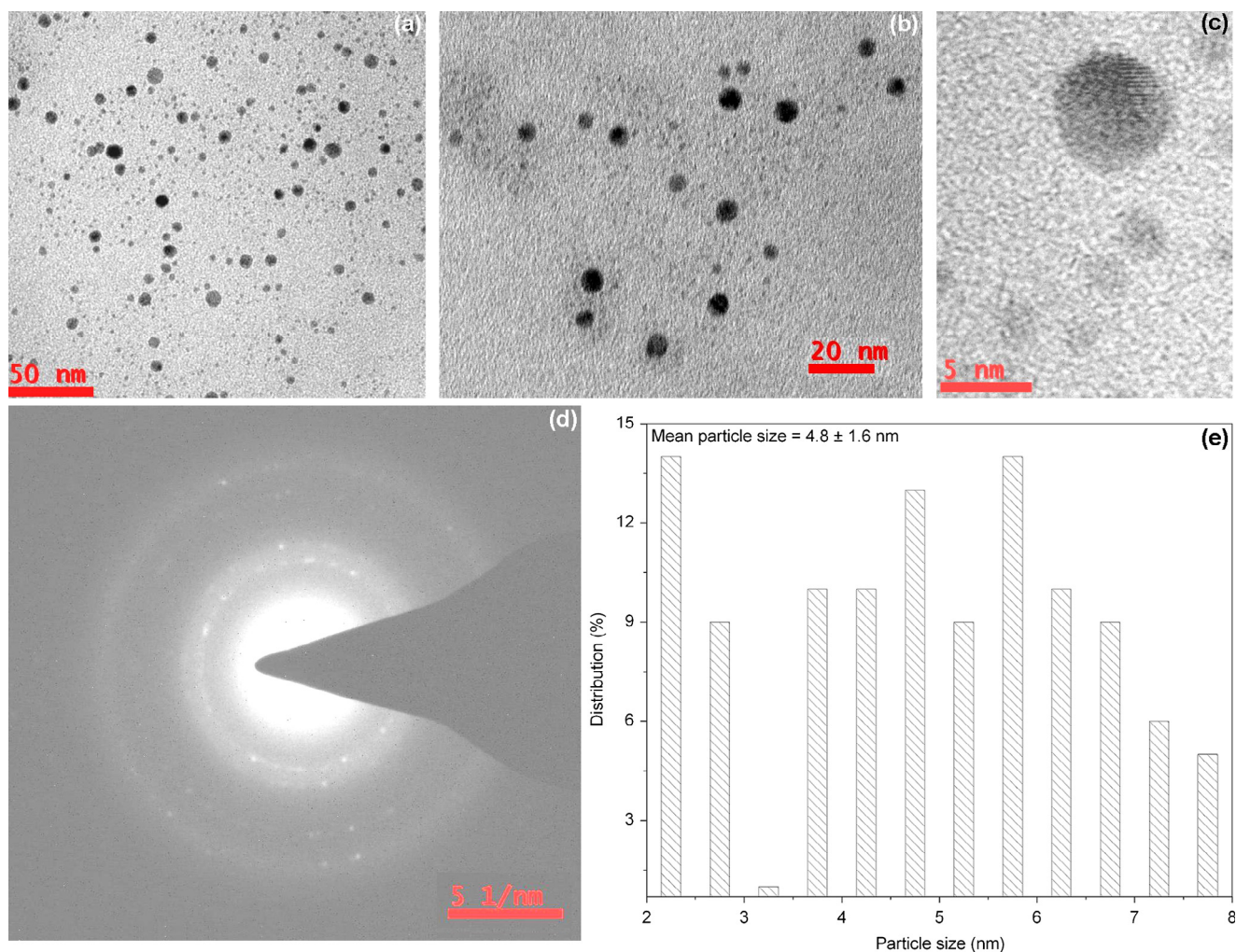


**Figure 4** The TEM image of palladium nanoparticles synthesized with 0.5% gum, 0.75 mM PdCl<sub>2</sub> and 30 min of autoclaving, at (a) 50 nm, (b) 20 nm and (c) 5 nm scale. (d) Corresponding SAED pattern and (e) histogram showing the particle size distribution.

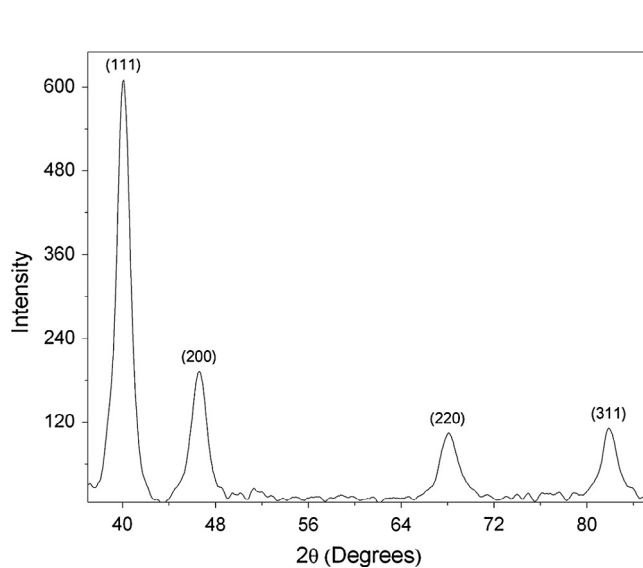


**Figure 5** X-ray diffraction pattern of lyophilized palladium nanoparticles, revealing the face centred cubic (fcc) crystal structure.

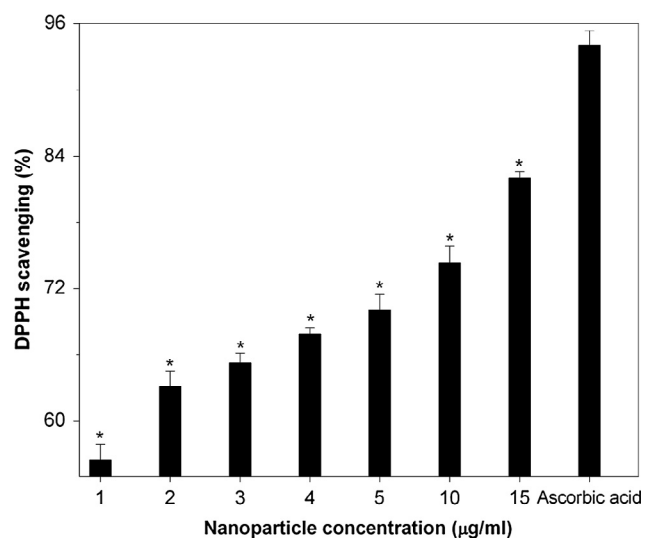


**Figure 6** The DPPH radical scavenging activity of palladium nanoparticles at different concentrations (1–15 µg/mL). Values are mean  $\pm$  SD for  $n = 3$ ; \*  $p < 0.0001$  compared to the positive control, ascorbic acid.

**Table 2** Comparison of DPPH scavenging activity of metal and metal oxide nanoparticles.

Nanoparticles	Concentration	Average size (nm)	DPPH scavenging (%)	References
Palladium	15 $\mu\text{g/mL}$	4.8	81.9	Present study
Gold	250 $\mu\text{g/mL}$	5–50	50	Ramamurthy et al. (2013)
Silver	250 $\mu\text{g/mL}$	5–50	55	Ramamurthy et al. (2013)
Selenium	4 mg/mL	34.9	85.3	Kong et al. (2014)
Copper oxide	37.5 mg/mL	15–30	85	Das et al. (2013)
Nickel oxide	33.3 mg/mL	12–23	90	Saikia et al. (2010)

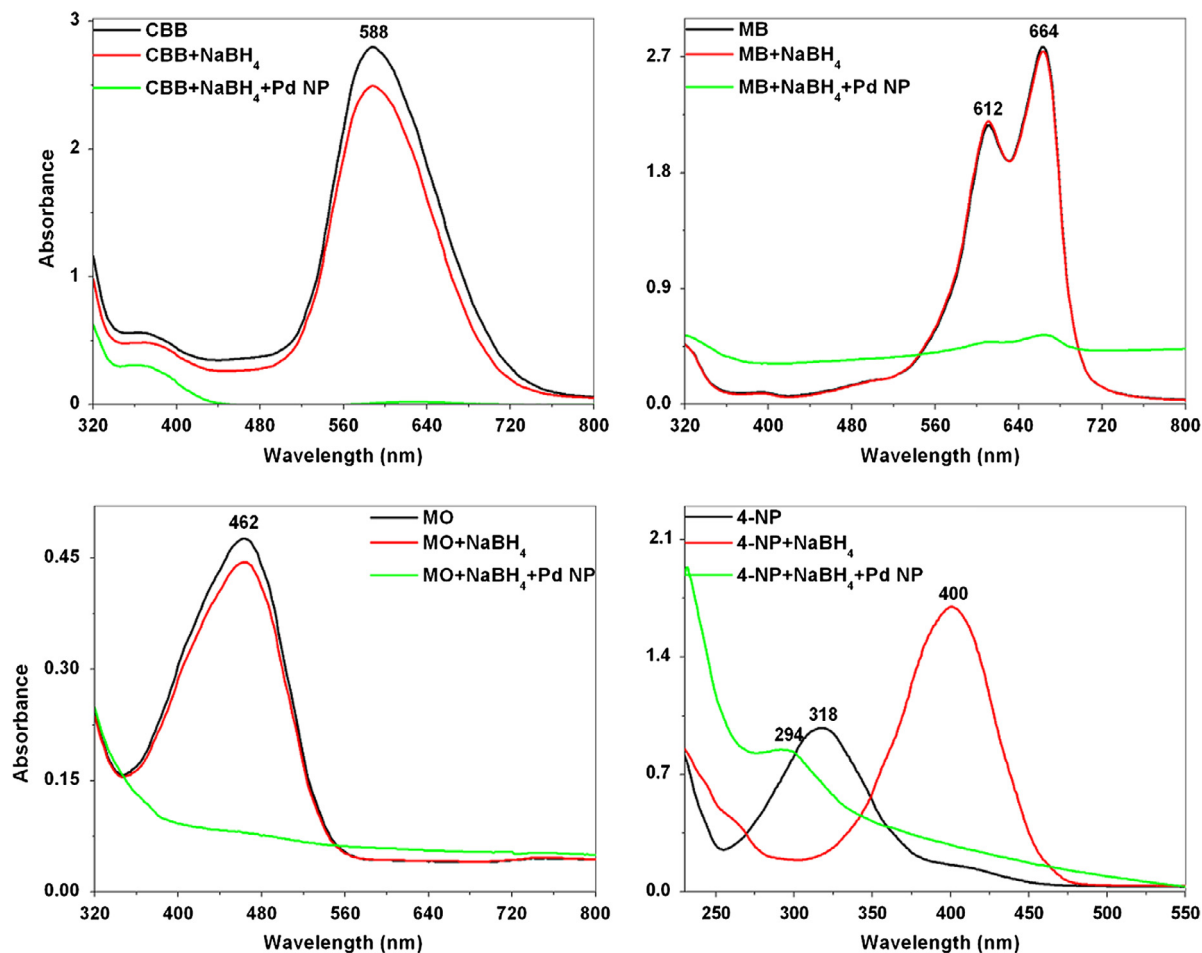


**Figure 7** The UV-vis spectra of dye reduction by  $\text{NaBH}_4$  (12.5 mM) using 3.2  $\mu\text{g/mL}$  of palladium nanoparticles (Pd NP) as catalyst at 2 min. (a) Coomassie brilliant blue G-250 (150  $\mu\text{M}$ ), (b) methylene blue (62.5  $\mu\text{M}$ ), (c) methyl orange (30  $\mu\text{M}$ ) and (d) 4-nitrophenol (100  $\mu\text{M}$ ).

antioxidant activity of gum ghatti reduced palladium nanoparticles at a much lower nanoparticle dose.

### 3.6. Catalytic activity

The catalytic degradation of coomassie brilliant blue G-250 (CBB) at 150  $\mu\text{M}$  concentration (500  $\mu\text{M}$ –300  $\mu\text{L}$ ) was investigated by monitoring the characteristic absorption peak at 588 nm, during palladium nanoparticle catalysed borohydride reduction. Within 2 min, CBB was decolorized by 3.2  $\mu\text{g/mL}$  of nanoparticles at 12.5 mM of  $\text{NaBH}_4$ . The progress of the reaction was very slow in the absence of nanocatalyst

(Fig. 7(a)). Whereas, control experiments carried out with gum and  $\text{NaBH}_4$  did not exhibit any catalytic activity. Similarly, the catalytic potential of the produced nanoparticles (3.2  $\mu\text{g/mL}$ ) in the reduction of methylene blue, a hetero-polyaromatic dye at 62.5  $\mu\text{M}$  concentration (250  $\mu\text{M}$ –250  $\mu\text{L}$ ) by  $\text{NaBH}_4$  (12.5 mM) was studied (Kalaiselvi et al.). The disappearance of MB characteristic absorption peak at 664 nm along with a shoulder at 612 nm was noted within 2 min, with a colour change from blue to colourless, thus, indicating the complete reduction of the dye to leuco methylene blue. In the absence of catalyst,  $\text{NaBH}_4$  alone was not able to reduce the MB (Fig. 7(b)). The catalytic activity of the generated

nanoparticles was also studied at room temperature by probing the borohydride reduction of methyl orange (MO), a mutagenic azo dye at 30  $\mu\text{M}$  concentration (100  $\mu\text{M}$ –300  $\mu\text{L}$ ). The characteristic absorption peak of MO observed at 462 nm was disappeared within 2 min in the presence of nanoparticle catalyst and  $\text{NaBH}_4$ . While, the  $\text{NaBH}_4$  mediated dye degradation was very poor in the absence of catalyst (Fig. 7(c)).

The catalytic activity of Pd NP (3.2  $\mu\text{g}/\text{mL}$ ) was evaluated by the reduction of 100  $\mu\text{M}$  (1000  $\mu\text{M}$ –100  $\mu\text{L}$ ) of 4-nitrophenol (4-NP), a carcinogenic dye into 4-aminophenol (4-AP) by 12.5 mM of  $\text{NaBH}_4$ . The reduction was monitored by recording the absorption spectrum from 250 to 550 nm for 2 min. After the addition of  $\text{NaBH}_4$ , the initial absorption peak of 4-NP at 318 nm was red shifted to 400 nm, due to the production of 4-nitrophenolate ion under alkaline conditions (Fig. 7(d)). In the absence of the palladium nanocatalyst, the absorption maximum of 4-NP and  $\text{NaBH}_4$  remains unaffected by time. But, after the addition of nanoparticles, the absorption intensity of 4-NP at 400 nm rapidly reduced with time and a new peak at 294 nm appeared concurrently. The appearance of the characteristic peak at 294 nm indicates the reduction of 4-NP to 4-AP (Fig. 7(d)). The entire reduction

reaction was substantiated by a concomitant colour change from yellow to colourless. Despite the fact that, the reduction of various dyes by sodium borohydride in aqueous medium is thermodynamically favoured, it is kinetically hindered. This kinetic barrier is mainly due to the large potential difference between donor and acceptor molecules. While in the presence of nanoparticles, both the substrates will be adsorbed on the particle surface and the nanoparticles facilitate the transfer of electrons from the reductant borohydride to the oxidant molecules. From the data, it is evident that the palladium nanoparticles act as a redox catalyst by decreasing the activation energy of the chemical reaction, via electron relay effect (Kalaiselvi et al., 2015). The rate constant,  $k$  was calculated for the reduction of 4-NP catalysed by palladium nanoparticles and obtained a rate constant of 0.11  $\text{min}^{-1}$  only at 3.2  $\mu\text{g}/\text{mL}$  of nanoparticles. The rate constant for the synthesized catalyst towards 4-NP reduction was compared with other reported catalysts of silver, gold and palladium nanoparticles (Table 3). From the data it is apparent, the studied activity is size dependent and the palladium nanoparticles exhibited enhanced catalytic activity compared to silver and gold nanoparticles, which is due to the smaller particle size of gum reduced palladium nanoparticles. The activity of the studied catalyst was comparable with other reported palladium nanoparticles.

**Table 3** Comparison of rate constants for the reduction of 4-nitrophenol using different nanoparticles.

Nanoparticles	Average size (nm)	Rate constant ( $\text{min}^{-1}$ )	References
Palladium	4.8	0.11	Present study
Silver	25	0.067	Narayanan et al. (2013)
Silver	15	0.07	Bindhu and Umadevi (2015)
Silver	10	0.1	Kundu (2013)
Gold	25	0.026	Narayanan and Sakthivel (2011)
Gold	15	0.019	Sen et al. (2013)
Gold	6.9	0.027	Maity et al. (2012)
Palladium	10	0.183	Santoshi kumari et al. (2015)
Palladium	2–4	0.117	Dauthal and Mukhopadhyay (2013)

### 3.7. Antibacterial activity

The well diffusion method was used to study the antibacterial action of the synthesized nanoparticles. After 24 h of incubation at 37  $^{\circ}\text{C}$ , growth suppression was not observed in plates loaded with 10  $\mu\text{g}$  of nanoparticles and negative control plates loaded with autoclaved gum. Whereas, the positive control plates loaded with 10  $\mu\text{g}$  of streptomycin antibiotic exhibited 14.3  $\pm$  1.5 and 12  $\pm$  0 mm ZOI against Gram-negative *P. aeruginosa* 27853 and Gram-positive *S. aureus* 25923, respectively (Fig. 8). The results of this study indicate that the produced palladium nanoparticles were not antibacterial. Thus, the nanoparticles may be employed as non-antibacterial, environmental friendly catalysts for dye degradation.

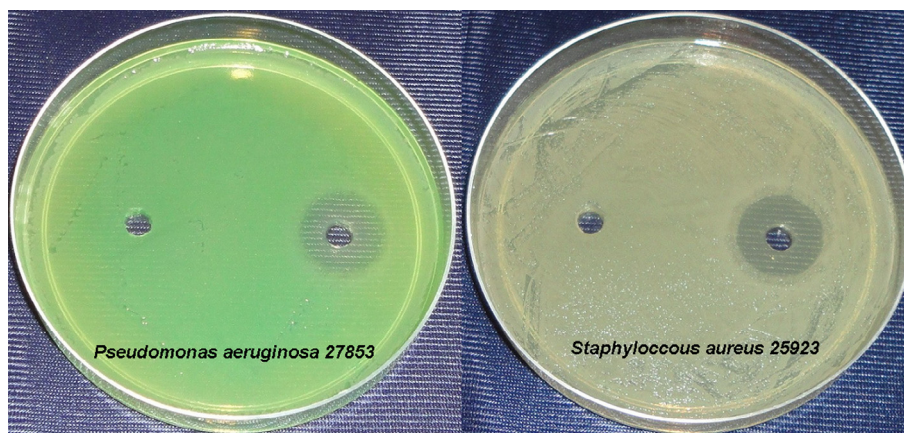


**Figure 8** Bacterial culture plates showing the inhibition zones around the loaded wells. Left well: 10  $\mu\text{g}$  of palladium nanoparticles and right well: 10  $\mu\text{g}$  of streptomycin.

#### 4. Conclusions

A simple green chemistry based single pot method for the synthesis of palladium nanoparticles was developed using arabinogalactan polymer, gum ghatti. The synthesis and stabilization of the crystalline, spherical nanoparticles of 4.8 nm was mediated by the hydroxyl and carboxylate groups and proteins of the gum, respectively. The biogenic nanoparticles were non-toxic to bacteria and exhibited enhanced antioxidant and catalytic activities. In particular, the dye degradation capability of the nanoparticles can have vast applications in eco-friendly environmental remediation of organic compounds.

#### Acknowledgements

The authors would like to thank Dr. D. Karunasagar, Head, EACS and Dr. Sunil Jai Kumar, Head, NCCCM/BARC for their constant support and encouragement throughout the work.

#### References

- Amar, V., Al-Assaf, S., Phillips, G.O., 2006. An introduction to gum ghatti: another proteinaceous gum. *Foods Food Ingredients J.* 211 (3), 275–280.
- Anastas, P.T., Warner, J.C., 1998. *Green Chemistry: Theory and Practice*. Oxford University Press, New York, pp. 30.
- Bankar, A., Joshi, B., Kumar, A.R., Zinjarde, S., 2010. Banana peel extract mediated novel route for the synthesis of palladium nanoparticles. *Mater. Lett.* 64 (18), 1951–1953.
- Bindhu, M.R., Umadevi, M., 2015. Antibacterial and catalytic activities of green synthesized silver nanoparticles. *Spectrochim. Acta Part A* 135, 373–378.
- Coccia, F., Tonucci, L., Bosco, D., Bressan, M., d'Alessandro, N., 2012. One-pot synthesis of lignin-stabilised platinum and palladium nanoparticles and their catalytic behaviour in oxidation and reduction reactions. *Green Chem.* 14 (4), 1073–1078.
- Das, D., Nath, B.C., Phukon, P., Dolui, S.K., 2013. Synthesis and evaluation of antioxidant and antibacterial behavior of CuO nanoparticles. *Colloids Surf. B* 101, 430–433.
- Dauthal, P., Mukhopadhyay, M., 2013. Biosynthesis of palladium nanoparticles using *Delonix regia* leaf extract and its catalytic activity for nitro-aromatics hydrogenation. *Ind. Eng. Chem. Res.* 52 (51), 18131–18139.
- Hakamada, M., Furukawa, T., Yamamoto, T., Takahashi, M., Mabuchi, M., 2011. Abnormal hydrogen absorption/desorption properties of nanoporous Pt with large lattice strains. *Mater. Trans.* 52 (4), 806–809.
- Hsu, W.-H., Jiang, S.-J., Sahayam, A.C., 2013. Determination of Cu, As, Hg and Pb in vegetable oils by electrothermal vaporization inductively coupled plasma mass spectrometry with palladium nanoparticles as modifier. *Talanta* 117, 268–272.
- Iravani, S., 2011. Green synthesis of metal nanoparticles using plants. *Green Chem.* 13 (10), 2638–2650.
- Kalaiselvi, A., Roopan, S.M., Madhumitha, G., Ramalingam, C., Elango, G., 2015. Synthesis and characterization of palladium nanoparticles using *Catharanthus roseus* leaf extract and its application in the photo-catalytic degradation. *Spectrochim. Acta Part A* 135, 116–119.
- Kanchana, A., Devarajan, S., Ayyappan, S.R., 2010. Green synthesis and characterization of palladium nanoparticles and its conjugates from *Solanum trilobatum* leaf extract. *Nano-Micro Lett.* 2 (2), 169–176.
- Kaur, L., Singh, J., Singh, H., 2009. Characterization of gum ghatti (*Anogeissus latifolia*): a structural and rheological approach. *J. Food Sci.* 74 (6), E328–E332.
- Kim, S.-W., Kim, M., Lee, W.Y., Hyeon, T., 2002. Fabrication of hollow palladium spheres and their successful application to the recyclable heterogeneous catalyst for Suzuki coupling reactions. *J. Am. Chem. Soc.* 124 (26), 7642–7643.
- Kong, H., Yang, J., Zhang, Y., Fang, Y., Nishinari, K., Phillips, G.O., 2014. Synthesis and antioxidant properties of gum arabic-stabilized selenium nanoparticles. *Int. J. Biol. Macromol.* 65, 155–162.
- Kora, A.J., Sashidhar Rao, B., Jayaraman, A., 2012. Size-controlled green synthesis of silver nanoparticles mediated by gum ghatti (*Anogeissus latifolia*) and its biological activity. *Org. Med. Chem. Lett.* 2 (1), 1–10.
- Kundu, S., 2013. Formation of self-assembled Ag nanoparticles on DNA chains with enhanced catalytic activity. *Phys. Chem. Chem. Phys.* 15 (33), 14107–14119.
- Kundu, S., Liang, H., 2011. Shape-selective formation and characterization of catalytically active iridium nanoparticles. *J. Colloid Interface Sci.* 354 (2), 597–606.
- Lengke, M.F., Fleet, M.E., Southam, G., 2007. Synthesis of palladium nanoparticles by reaction of filamentous cyanobacterial biomass with a palladium(II) chloride complex. *Langmuir* 23 (17), 8982–8987.
- Lishan, J., Qian, Z., Qingbiao, L., Hao, S., 2009. The biosynthesis of palladium nanoparticles by antioxidants in *Gardenia jasminoides Ellis*: long lifetime nanocatalysts for p-nitrotoluene hydrogenation. *Nanotechnology* 20 (38), 385601.
- Maity, S., Kumar Sen, I., Sirajul Islam, S., 2012. Green synthesis of gold nanoparticles using gum polysaccharide of *Cochlospermum religiosum* (katira gum) and study of catalytic activity. *Physica E* 45, 130–134.
- Meena Kumari, M., Aromal, S.A., Philip, D., 2013. Synthesis of monodispersed palladium nanoparticles using tannic acid and its optical non-linearity. *Spectrochim. Acta Part A* 103, 130–133.
- Mubeen, S., Zhang, T., Yoo, B., Deshusses, M.A., Myung, N.V., 2007. Palladium nanoparticles decorated single-walled carbon nanotube hydrogen sensor. *Phys. Chem. C* 111 (17), 6321–6327.
- Narayanan, K.B., Park, H.H., Sakthivel, N., 2013. Extracellular synthesis of mycogenic silver nanoparticles by *Cylindrocladium floridanum* and its homogeneous catalytic degradation of 4-nitrophenol. *Spectrochim. Acta Part A* 116, 485–490.
- Narayanan, K.B., Sakthivel, N., 2011. Synthesis and characterization of nano-gold composite using *Cylindrocladium floridanum* and its heterogeneous catalysis in the degradation of 4-nitrophenol. *J. Hazard. Mater.* 189 (1–2), 519–525.
- Ogi, T., Honda, R., Tamaoki, K., Saitoh, N., Konishi, Y., 2011. Direct room-temperature synthesis of a highly dispersed Pd nanoparticle catalyst and its electrical properties in a fuel cell. *Powder Technol.* 205 (1–3), 143–148.
- Praharaj, S., Nath, S., Ghosh, S.K., Kundu, S., Pal, T., 2004. Immobilization and recovery of Au nanoparticles from anion exchange resin: resin-bound nanoparticle matrix as a catalyst for the reduction of 4-nitrophenol. *Langmuir* 20 (23), 9889–9892.
- Ramamurthy, C.H., Padma, M., Mariya samadanam, I.D., Mareeswaran, R., Suyavaran, A., Kumar, M.S., Premkumar, K., Thirunavukkarasu, C., 2013. The extra cellular synthesis of gold and silver nanoparticles and their free radical scavenging and antibacterial properties. *Colloids Surf. B* 102, 808–815.
- Rao, C.R.K., Lakshminarayanan, V., Trivedi, D.C., 2006. Synthesis and characterization of lower size, laurylamine protected palladium nanoparticles. *Mater. Lett.* 60 (25–26), 3165–3169.
- Raut, R.W., Haroon, A.S.M., Malghe, Y.S., Nikam, B.T., Kashid, S.B., 2013. Rapid biosynthesis of platinum and palladium metal nanoparticles using root extract of *Asparagus racemosus* Linn. *Adv. Mater. Lett.* 4 (8), 650–654.
- Roopan, S.M., Bharathi, A., Kumar, R., Khanna, V.G., Prabhakarn, A., 2012. Acaricidal, insecticidal, and larvicidal efficacy of aqueous

- extract of *Annona squamosa* L peel as biomaterial for the reduction of palladium salts into nanoparticles. *Colloids Surf. B* 92, 209–212.
- Saikia, J.P., Paul, S., Konwar, B.K., Samdarshi, S.K., 2010. Nickel oxide nanoparticles: a novel antioxidant. *Colloids Surf. B* 78 (1), 146–148.
- Santoshi kumari, A., Venkatesham, M., Ayodhya, D., Veerabhadram, G., 2015. Green synthesis, characterization and catalytic activity of palladium nanoparticles by xanthan gum. *Appl. Nanosci.* 5 (3), 315–320.
- Sathishkumar, M., Sneha, K., Kwak, I.S., Mao, J., Tripathy, S.J., Yun, Y.S., 2009. Phyto-crystallization of palladium through reduction process using *Cinnamom zeylanicum* bark extract. *J. Hazard. Mater.* 171 (1–3), 400–404.
- Sen, I.K., Maity, K., Islam, S.S., 2013. Green synthesis of gold nanoparticles using a glucan of an edible mushroom and study of catalytic activity. *Carbohydr. Polym.* 91 (2), 518–528.
- Sheny, D.S., Philip, D., Mathew, J., 2012. Rapid green synthesis of palladium nanoparticles using the dried leaf of *Anacardium occidentale*. *Spectrochim. Acta Part A* 91, 35–38.
- Tischer, C.A., Iacomini, M., Wagner, R., Gorin, P.A.J., 2002. New structural features of the polysaccharide from gum ghatti (*Anogeissus latifolia*). *Carbohydr. Res.* 337 (21–23), 2205–2210.
- Tuo, Y., Liu, G., Zhou, J., Wang, A., Wang, J., Jin, R., Lv, H., 2013. Microbial formation of palladium nanoparticles by *Geobacter sulfurreducens* for chromate reduction. *Bioresour. Technol.* 133, 606–611.